Chapter 3

A robust adaptive numerical method for singularly perturbed parabolic reaction-diffusion problems with Robin boundary conditions

In this chapter, we consider a singularly perturbed time-dependent reaction-diffusion problem with Robin boundary conditions (RBCs). Let the domain be $\bar{G} = G \cup \partial G$, where $G := G_x \times (0, T]$ with $G_x = (0, 1)$. Suppose $\partial G = \Gamma_b \cup \Gamma_r \cup \Gamma_l$ with $\Gamma_b = [0, 1]\times\{0\}$, $\Gamma_l = \{0\} \times (0, T]$, and $\Gamma_r = \{1\} \times (0, T]$. On this domain we define the model problem as follows

$$\begin{cases} \mathcal{L}y(x,t) := \frac{\partial y}{\partial t}(x,t) + \mathcal{L}_\varepsilon y(x,t) = f(x,t), \ (x,t) \in G, \\ \mathcal{D}_l y(0,t) := y(0,t) - \sqrt{\varepsilon}\frac{\partial y}{\partial x}(0,t) = \phi_l(t), \ t \in (0,T], \\ \mathcal{D}_r y(1,t) := y(1,t) + \sqrt{\varepsilon}\frac{\partial y}{\partial x}(1,t) = \phi_r(t), \ t \in (0,T], \\ y(x,0) = \phi_b(x), \ x \in \bar{G}_x, \end{cases} \tag{3.1}$$

where $\mathcal{L}_\varepsilon y(x,t) := -\varepsilon\frac{\partial^2 y}{\partial x^2}(x,t)+a(x)y(x,t)$ and $0 < \varepsilon \leq 1$ is a small positive constant called the perturbation parameter. The functions $a(x)$ and $f(x,t)$ are assumed to be sufficiently smooth on their respective domains, with $0 < \alpha \leq a(x)$ on $\bar{G}_x$. It is known that the solution exhibits layers near the boundaries $x = 0$ and $x = 1$, and further the solution $y(x,t)$ can be decomposed as a sum of a regular part v and a

singular part w , satisfying [98, 117]

$$\left\| \frac{\partial^{p+q} y}{\partial x^p \partial t^q} \right\|_{\bar{G}} < C\varepsilon^{-\frac{p}{2}}, \quad \text{for } 1 \le p+2q \le 4,\ p,q \in \mathbb{N}_0, \tag{3.2}$$

$$\left\| \frac{\partial^{p+q} v}{\partial x^p \partial t^q} \right\|_{\bar{G}} < C, \quad \text{for } 1 \le p+2q \le 4,\ p,q \in \mathbb{N}_0, \tag{3.3}$$

$$\text{and} \quad \left| \frac{\partial^{p+q} w}{\partial x^p \partial t^q} \right|_{\bar{G}} < C\varepsilon^{-\frac{p}{2}} (e^{-x\sqrt{\frac{\alpha}{\varepsilon}}} + e^{-(1-x)\sqrt{\frac{\alpha}{\varepsilon}}}), \quad \text{for } 1 \le p+2q \le 4,\ p,q \in \mathbb{N}_0. \tag{3.4}$$

Singularly perturbed problems similar to (3.1) with Dirichlet type boundary conditions have been studied extensively in the literature (see [34, 83, 85, 93, 118–121] and the references therein). However, there are only few studies of such problems with Robin boundary conditions (RBCs) [98, 117, 122, 123]. Note that all of these studies considered Shishkin meshes to resolve the layers and to develop parameter-robust numerical methods. As per our knowledge, in the literature there is no result considering the approximation of a time-dependent problem with Robin boundary conditions on layer-adaptive equidistributed meshes. So, in this chapter, we construct a parameter-robust numerical method on equidistributed meshes for problem (3.1). We generate the adaptive mesh at each time level based on a suitable monitor function $\mathcal{M}$. The time derivative is discretized by a modified Euler scheme, the space derivative is discretized by the central difference scheme, and the Robin boundary conditions are approximated by a special finite difference scheme to maintain the accuracy. We provide convergence analysis of the proposed method and prove that the method is parameter-robust convergent of first order in time and second order in space. Some numerical experiments are conducted in order to validate our theoretical results and demonstrate the effectiveness of the method.

This chapter is structured as follows: The problem discretization and the adaptive mesh formation are given in Section 3.1. Section 3.2 is devoted to the analysis of a

stationary version of problem (3.1). In Section 3.3, the error analysis of the proposed method is done. Section 3.4 is devoted to the results and discussion of numerical experiments for two test examples. Then the chapter concludes with Section 3.5.

3.1 Discretization and adaptive mesh generation

3.1.1 The discretization strategy

In time direction we take a uniform mesh $\{t_j\}_{j=0}^{M}$ with step size $\Delta t = T/M$, where M is the number of mesh intervals. Then an arbitrary non-uniform spatial mesh is considered at any time level t_j denoted by $\{x_i^j\}_{i=0}^{N}$ with step sizes $h_i^j = x_i^j - x_{i-1}^j,\ i = 1, \ldots, N$. Thus, the complete discretization of the domain is the tensor product of these two one-dimensional meshes. On this discrete domain, problem (3.1) is discretized by

$$\begin{cases} [L^{N,M}Y]_i^j := \delta_t^\star Y_i^j + [L_\varepsilon^{N,M}Y]_i^j = f_i^j,\ i = 1, ..., N-1,\ j = 1, ..., M, \\ [D_l^{N,M}Y]_0^j := Y_0^j - \sqrt{\varepsilon} D_x^+ Y_0^j + \frac{h_1^j}{2\sqrt{\varepsilon}}(a_0 Y_0^j + \delta_t^\star Y_0^j) = \phi_l^j + \frac{h_1^j}{2\sqrt{\varepsilon}} f_0^j,\ j = 1, ..., M, \\ [D_r^{N,M}Y]_N^j := Y_N^j + \sqrt{\varepsilon} D_x^- Y_N^j + \frac{h_N^j}{2\sqrt{\varepsilon}}(a_N Y_N^j + \delta_t^\star Y_N^j) = \phi_r^j + \frac{h_N^j}{2\sqrt{\varepsilon}} f_N^j,\ j = 1, ..., M, \\ Y_i^0 = \phi_{b;i}, \quad i = 0, ..., N, \end{cases} \tag{3.5}$$

where

$$[L_\varepsilon^{N,M}Y]_i^j := -\varepsilon \delta_x^2 Y_i^j + a_i Y_i^j, \quad \delta_t^\star Y_i^j = \frac{Y_i^j - \widetilde{Y}_i^{j-1}}{\Delta t},$$

$$D_x^+ Y_i^j = \frac{Y_{i+1}^j - Y_i^j}{h_{i+1}^j}, \quad D_x^- Y_i^j = \frac{Y_i^j - Y_{i-1}^j}{h_i^j}, \quad \delta_x^2 Y_i^j = \frac{(D_x^+ - D_x^-)Y_i^j}{(h_i^j + h_{i+1}^j)/2},$$

$a_i = a(x_i^j), f_i^j = f(x_i^j, t_j),\ \phi_{b;i} = \phi_b(x_i^j)$, and $\widetilde{Y}_i^{j-1}$ represents the linear interpolant of $Y_i^{j-1} = Y(x_i^{j-1}, t_{j-1}),\ 0 \le i \le N$, at the point x_i^j. We also define $[D_{r,x}^{N,M}Y]_N^j :=$

$Y_N^j + \sqrt{\varepsilon} D_x^- Y_N^j + \frac{h_N^j}{2\sqrt{\varepsilon}} a_N Y_N^j$ and $[D_{l,x}^{N,M} Y]_0^j := Y_0^j - \sqrt{\varepsilon} D_x^+ Y_0^j + \frac{h_1^j}{2\sqrt{\varepsilon}} a_0 Y_0^j$, that we shall use later in Section 3.17. Using standard arguments we can prove that the following discrete maximum principle holds [98].

Lemma 3.1.1. (Discrete maximum principle) Consider a mesh function U such that $[L^{N,M}U]_i^j \geq 0$ for $i = 1, ..., N-1,\ j = 1, ..., M$, and $[D_l^{N,M}U]_0^j \geq 0,\ [D_r^{N,M}U]_N^j \geq 0$ for $j = 1, ..., M$. Then $U_i^j \geq 0$ for $i = 0, ..., N,\ j = 0, ..., M$.

3.1.2 Layer-adaptive equidistribution mesh

The solution of problem (3.1) possesses boundary layers, so we need a layer resolving mesh in the spatial direction. We here construct the layer resolving mesh using the equidistribution principle. At any time level t_k, the mesh $\{x_i^k\}_{i=0}^N$ is said to be equidistributed with respect to the monitor function $\mathcal{M}(y(x,t_k),x)$ if

$$\int_{x_{i-1}^k}^{x_i^k} \mathcal{M}(y(z,t_k),z)dz = \frac{1}{N}\int_0^1 \mathcal{M}(y(z,t_k),z)dz, \quad 1 \leq i \leq N. \tag{3.6}$$

The following monitor function is considered

$$\mathcal{M}(y(x,t_k),x) = \aleph^k + \left|\frac{\partial^2 w}{\partial x^2}(x,t_k)\right|^{1/2}, \tag{3.7}$$

where $\aleph^k$ is chosen according to the specifications in Lemma 3.1.2, below. A similar monitor function is also considered in [56, 59] for problems with Dirichlet boundary conditions. Using this monitor function, the equidistributed mesh at any time t_k is obtained by using the following relation

$$\int_0^{x^k(\xi)} \mathcal{M}(y(z,t_k),z)dz = \xi\int_0^1 \mathcal{M}(y(z,t_k),z)dz, \quad \xi \in [0,1], \tag{3.8}$$

which is equivalent to (3.6). To get the structure of the mesh generated using (3.8), we follow the similar approach as in [56, 113]. Consider the derivative bounds of w from (3.4) to approximate $\frac{\partial^2 w}{\partial x^2}$ as

$$\frac{\partial^2 w}{\partial x^2}(x,t_k) \approx \begin{cases} \frac{\nu_1}{\varepsilon} e^{-x\sqrt{\frac{\alpha}{\varepsilon}}}, & x \in [0,1/2], \\ \frac{\nu_2}{\varepsilon} e^{-(1-x)\sqrt{\frac{\alpha}{\varepsilon}}}, & x \in (1/2,1], \end{cases}$$

where ν_1 and ν_2 are constants, independent of ε and x. So,

$$\int_0^1 \left|\frac{\partial^2 w}{\partial x^2}(z,t_k)\right|^{1/2} dz \equiv \mathbf{A} \approx 2\left[\frac{|\nu_1|^{1/2}+|\nu_2|^{1/2}}{\alpha^{1/2}}\right].$$

Hence, from (3.7) and (3.8), for $x^k(\xi) \le \frac{1}{2}$, we have the mapping

$$\xi\left(\frac{\aleph^k}{\mathbf{A}}+1\right) = \frac{\aleph^k}{\mathbf{A}} x^k(\xi) + \lambda_1\left(1 - e^{-\frac{x^k(\xi)}{2}\sqrt{\frac{\alpha}{\varepsilon}}}\right), \tag{3.9}$$

where

$$\lambda_1 = \frac{|\nu_1|^{1/2}}{|\nu_1|^{1/2}+|\nu_2|^{1/2}}.$$

Similarly, for $x^k(\xi) > \frac{1}{2}$, the equidistribution principle gives

$$(1-\xi)\left(\frac{\aleph^k}{\mathbf{A}}+1\right) = \frac{\aleph^k}{\mathbf{A}}(1-x^k(\xi)) + \lambda_2\left(1 - e^{-\frac{1-x^k(\xi)}{2}\sqrt{\frac{\alpha}{\varepsilon}}}\right), \tag{3.10}$$

where

$$\lambda_2 = \frac{|\nu_2|^{1/2}}{|\nu_1|^{1/2}+|\nu_2|^{1/2}}.$$

Thus, corresponding to a uniform mesh $\{\xi_i = i/N\}_{i=0}^N$ in computational space we obtain a non-uniform mesh $\{x_i^k\}_{i=0}^N$ in physical space at each time level using the following relations

$$\frac{i}{N}\left(\frac{\aleph^k}{\mathbf{A}}+1\right) = \frac{\aleph^k}{\mathbf{A}} x_i^k + \lambda_1\left(1 - e^{-\frac{x_i^k}{2}\sqrt{\frac{\alpha}{\varepsilon}}}\right), \quad x_i^k \le 1/2 \tag{3.11}$$

and

$$(1-\frac{i}{N})(\frac{\aleph^k}{\mathbf{A}}+1)=\frac{\aleph^k}{\mathbf{A}}(1-x_i^k)+\lambda_2(1-e^{-\frac{(1-x_i^k)}{2}\sqrt{\frac{\alpha}{\varepsilon}}}), \quad x_i^k>1/2. \tag{3.12}$$

The following lemma provides information about the distribution of the mesh points and also gets some bounds on the mesh spacing.

Lemma 3.1.2. Taking $\aleph^k=\mathbf{A}$, the non-uniform mesh generated by (3.11) and (3.12) satisfies

$$x_\ell^k<2\sqrt{\frac{\varepsilon}{\alpha}}\log N<x_{\ell+1}^k \quad \text{and} \quad x_{r-1}^k<1-2\sqrt{\frac{\varepsilon}{\alpha}}\log N<x_r^k, \tag{3.13}$$

where

$$\ell=\left[\frac{1}{2}\left(2\sqrt{\frac{\varepsilon}{\alpha}}N\log N+\lambda_1(N-1)\right)\right], \quad r=\left[N-\frac{1}{2}\left(2\sqrt{\frac{\varepsilon}{\alpha}}N\log N+\lambda_2(N-1)\right)\right]+1$$

and $[\cdot]$ is the integer part function. Moreover, the mesh spacing satisfies

$$h_i^k<C\sqrt{\frac{\varepsilon}{\alpha}} \quad \text{for } i=1,...,\ell \text{ and } i=r+1,...,N-1 \tag{3.14}$$

with

$$|h_{i+1}^k-h_i^k|\le C(h_i^k)^2 \quad \text{for } i=1,...,\ell-1 \quad \text{and} \quad |h_{i+1}^k-h_i^k|\le C(h_{i+1}^k)^2, \tag{3.15}$$

for $i=r+1,...,N-1$. Further, we have

$$h_i^k\le CN^{-1} \quad \text{for } i=1,...,N. \tag{3.16}$$

Proof. The proof of (3.13)-(3.15) can be obtained using arguments similar to those in [56]. To prove (3.16), we shall work as is done in [90, 124]. Note that for the monitor

function (3.7) we have $\mathbf{A} = \aleph^k \leq \mathcal{M}(y(x,t_k),x)$. So, using derivative bounds we get

$$\int_0^1 \mathcal{M}(y(z,t_k),z)dz \leq C.$$

Thus, by the equidistribution principle, we get

$$\aleph^k h_i^k \leq \int_{x_{i-1}^k}^{x_i^k} \mathcal{M}(y(z,t_k),z)dz = \frac{1}{N}\int_0^1 \mathcal{M}(y(z,t_k),z)dz \leq CN^{-1}.$$

Hence, $h_i^k \leq CN^{-1}$. □

3.2 A stationary problem

The stationary version of problem (3.1) is an important ingredient needed to study the time dependent problem (3.1). So, this section is devoted to parameter-robust convergence analysis of a finite difference scheme (similar to (3.5)) on equidistributed meshes for the following stationary problem

$$\begin{cases} \mathcal{L}_\varepsilon y := -\varepsilon \frac{d^2y}{dx^2} + a(x)y = f(x), \quad x \in (0,1), \\ \mathcal{D}_{l,x}y(0) := y(0) - \sqrt{\varepsilon}\frac{dy}{dx}(0) = \phi_l, \\ \mathcal{D}_{r,x}y(1) := y(1) + \sqrt{\varepsilon}\frac{dy}{dx}(1) = \phi_r. \end{cases} \tag{3.17}$$

We assume that the functions $a(x)$ and $f(x)$ are sufficiently smooth and that $0 < \alpha \leq a(x)$, $x \in [0,1]$. This problem has been previously studied in [90], where y is decomposed as $y = v + w$, and the following bounds were obtained

$$\left|\frac{d^p v(x)}{dx^p}\right| \leq C(1+\varepsilon^{1-p/2}), \tag{3.18}$$

$$\left|\frac{d^p w(x)}{dx^p}\right| \leq C\varepsilon^{-\frac{p}{2}}(e^{-x\sqrt{\frac{\alpha}{\varepsilon}}} + e^{-(1-x)\sqrt{\frac{\alpha}{\varepsilon}}}),\ 0 \leq p \leq 4,\ x \in [0,1]. \tag{3.19}$$

A coupled system of two stationary problems with RBCs is studied in [124]. In [90, 124], for boundary conditions a scheme based on cubic splines is used and for interior points differential equation is discretized using the classical central difference scheme. But, here we discretize problem (3.17) using a scheme similar to (3.5). The discretization is as follows

$$\begin{cases} [L_\varepsilon^N Y]_i \coloneqq -\varepsilon\delta_x^2 Y_i + a_i Y_i = f_i, \quad i = 1, ..., N-1, \\ [D_{l,x}^N Y]_0 \coloneqq Y_0 - \sqrt{\varepsilon} D_x^+ Y_0 + \frac{h_1}{2\sqrt{\varepsilon}} a_0 Y_0 = \phi_l + \frac{h_1}{2\sqrt{\varepsilon}} f_0, \\ [D_{r,x}^N Y]_N \coloneqq Y_N + \sqrt{\varepsilon} D_x^- Y_N + \frac{h_N}{2\sqrt{\varepsilon}} a_N Y_N = \phi_r + \frac{h_N}{2\sqrt{\varepsilon}} f_N, \end{cases} \tag{3.20}$$

where the difference operators D_x^+, D_x^- and δ_x^2 defined analogously as for the discretization (3.5), and the mesh $\{x_i\}_{i=0}^N$ is the following equidistributed mesh with step sizes $h_i = x_i - x_{i-1}$,

$$\frac{i}{N}(\frac{\aleph}{\mathbf{A}} + 1) = \frac{\aleph}{\mathbf{A}} x_i + \lambda_1(1 - e^{-\frac{x_i}{2}\sqrt{\frac{\alpha}{\varepsilon}}}), \quad x_i \leq 1/2 \tag{3.21}$$

and

$$(1 - \frac{i}{N})(\frac{\aleph}{\mathbf{A}} + 1) = \frac{\aleph}{\mathbf{A}}(1 - x_i) + \lambda_2(1 - e^{-\frac{(1-x_i)}{2}\sqrt{\frac{\alpha}{\varepsilon}}}), \quad x_i > 1/2, \tag{3.22}$$

which is obtained using the monitor function $\mathcal{M} = \aleph + |\frac{d^2 w}{dx^2}|^{1/2}$ (see Section 3.1 for details). The discretization (3.20) satisfies the following discrete maximum principle which can be proved using standard arguments [98].

Lemma 3.2.1. (Discrete maximum principle) Consider a mesh function U such that $[L_\varepsilon^N U]_i \geq 0$ for $i = 1, ..., N-1$, and $[D_{l,x}^N U]_0 \geq 0$, $[D_{r,x}^N U]_N \geq 0$. Then $U_i \geq 0$ for $i = 0, ..., N$.

Theorem 3.2.1. Let y and Y be the solutions of (3.17) and (3.20), respectively. Then, for $i = 0, \ldots, N$, we have

$$|y(x_i) - Y_i| \leq CN^{-2}.$$

Proof. At the left boundary, we proceed as follows

$$\begin{aligned}
[D^N_{l,x}(y-Y)]_0 &= [D^N_{l,x}y]_0 - \left(\phi_l + \frac{h_1}{2\sqrt{\varepsilon}}f_0\right) \\
&= \left[y(x_0) - \sqrt{\varepsilon}D^+_x y(x_0) + \frac{h_1}{2\sqrt{\varepsilon}}a_0 y(x_0)\right] \\
&\qquad - \left[y(x_0) - \sqrt{\varepsilon}\frac{dy}{dx}(x_0) + \frac{h_1}{2\sqrt{\varepsilon}}f_0\right] \\
&= \sqrt{\varepsilon}\left(\frac{dy}{dx}(x_0) - D^+_x y(x_0)\right) + \frac{h_1}{2\sqrt{\varepsilon}}\big(a_0 y(x_0) - f_0\big) \\
&= \sqrt{\varepsilon}\left(\frac{dy}{dx}(x_0) - D^+_x y(x_0)\right) + \frac{h_1\sqrt{\varepsilon}}{2}\frac{d^2y}{dx^2}(x_0) \\
&= -\frac{h_1^2\sqrt{\varepsilon}}{6}\frac{d^3y}{dx^3}(\eta) \text{ for some } \eta \in (x_0, x_1).
\end{aligned}$$

Now using the solution decomposition we have

$$|[D^N_{l,x}(y-Y)]_0| = \frac{h_1^2\sqrt{\varepsilon}}{6}\left|\frac{d^3y}{dx^3}(\eta)\right| \leq \frac{h_1^2\sqrt{\varepsilon}}{6}\left|\frac{d^3v}{dx^3}(\eta)\right| + \frac{h_1^2\sqrt{\varepsilon}}{6}\left|\frac{d^3w}{dx^3}(\eta)\right|.$$

Using the derivative bounds of v from (3.18) and Lemma 3.1.2, we get

$$h_1^2\sqrt{\varepsilon}\frac{d^3v}{dx^3}(\eta) \leq CN^{-2}.$$

For layer component, we use derivative bounds from (3.19) and proceed as follows

$$\begin{aligned}
h_1^2\sqrt{\varepsilon}\frac{d^3w}{dx^3}(\eta) &\leq C\varepsilon^{-1}h_1^2 e^{-x_0\sqrt{\frac{\alpha}{\varepsilon}}} \\
&\leq C\varepsilon^{-1}\left(\int_{x_0}^{x_1} e^{-\frac{z}{2}\sqrt{\frac{\alpha}{\varepsilon}}}dz\right)^2 \leq C\varepsilon^{-1}\left(\sqrt{\varepsilon}\int_{x_0}^{x_1}\mathcal{M}(y(z),z)dz\right)^2 \\
&\leq C\mathbf{A}^2N^{-2} \leq CN^{-2}.
\end{aligned}$$

Hence

$$|[D^N_{l,x}(y-Y)]_0| \leq CN^{-2}. \tag{3.23}$$

Similarly

$$|[D^N_{r,x}(y-Y)]_N| \leq CN^{-2}. \tag{3.24}$$

We can use the arguments in [56] to show that

$$|[L^N_\varepsilon(y-Y)]_i| \leq CN^{-2} \quad \text{for } i = 1, ..., N-1. \tag{3.25}$$

Thus, we consider the barrier function $\Psi^\pm_i = CN^{-2} \pm (y(x_i) - Y_i)$ and use the discrete maximum principle (Lemma 3.2.1) to get the desired result. □

3.3 Error analysis

The parameter-robust convergence analysis of the difference scheme (3.5) is provided in the following theorem.

Theorem 3.3.1. Let $y(x^j_i, t_j)$ and Y^j_i be the solutions of (3.1) and (3.5), respectively. If for some $0 < \gamma < 1$ it is $N^{-\gamma} \leq C\Delta t$, then for $i = 0, \ldots, N,\ j = 0, \ldots, M$, we have the following bound

$$|y(x^j_i, t_j) - Y^j_i| \leq C(\Delta t + N^{-2+\gamma}).$$

Proof. Suppose $\eta^j_i = y(x^j_i, t_j) - Y^j_i$ denotes the error in the numerical solution at (x^j_i, t_j). So, we can write the truncation error as follows

$$[\delta^\star_t \eta]^j_i + [L^{N,M}_\varepsilon \eta]^j_i = \mathcal{X}^j_{1;i} + \mathcal{X}^j_{2;i}, \text{ for } i = 1, ..., N-1,\ j = 1, ..., M,$$

where

$$\mathcal{X}_{1;i}^j = [L_\varepsilon^{N,M} y]_i^j - (\mathcal{L}_\varepsilon y)_i^j \quad \text{and} \quad \mathcal{X}_{2;i}^j = \delta_t^\star y(x_i^j, t_j) - \frac{\partial y}{\partial t}(x_i^j, t_j).$$

Also,

$$[D_l^{N,M}\eta]_0^j = \zeta_{l,1;0}^j + \zeta_{l,2;0}^j,$$

$$[D_r^{N,M}\eta]_N^j = \zeta_{r,1;N}^j + \zeta_{r,2;N}^j,$$

where

$$\zeta_{l,1;0}^j = [D_{l,x}^{N,M} y]_0^j - \left((D_l y)_0^j + \frac{h_1^j}{2\sqrt{\varepsilon}} (\mathcal{L}_\varepsilon y)_0^j \right), \quad \zeta_{l,2;0}^j = \frac{h_1^j}{2\sqrt{\varepsilon}} (\delta_t^\star y(x_0^j, t_j) - \frac{\partial y}{\partial t}(x_0^j, t_j)),$$

$$\zeta_{r,1;N}^j = [D_{r,x}^{N,M} y]_N^j - \left((D_r y)_N^j + \frac{h_N^j}{2\sqrt{\varepsilon}} (\mathcal{L}_\varepsilon y)_N^j \right), \; \zeta_{r,2;N}^j = \frac{h_N^j}{2\sqrt{\varepsilon}} (\delta_t^\star y(x_N^j, t_j) - \frac{\partial y}{\partial t}(x_N^j, t_j)).$$

Now we split the error η_i^j as $\eta_i^j = \rho_i^j + \omega_i^j$, where ρ_i^j, for each fixed j, is the solution of the following stationary discrete problem

$$\begin{cases} [L_\varepsilon^{N,M}\rho]_i^j = \mathcal{X}_{1;i}^j, \; i = 1, ..., N-1, \\ [D_{l,x}^{N,M}\rho]_0^j = \zeta_{l,1;0}^j, \\ [D_{r,x}^{N,M}\rho]_N^j = \zeta_{r,1;N}^j, \end{cases} \tag{3.26}$$

and ω_i^j is the solution of the following parabolic discrete problem

$$\begin{cases} [\delta_t^\star \omega + L_\varepsilon^{N,M}\omega]_i^j = \mathcal{X}_{2;i}^j - \delta_t^\star \rho_i^j, \; i = 1, ..., N-1, \; j = 1, ..., M, \\ [D_l^{N,M}\omega]_0^j = \zeta_{l,2;0}^j - \frac{h_1^j}{2\sqrt{\varepsilon}} \delta_t^\star \rho_0^j, \; j = 1, ..., M, \\ [D_r^{N,M}\omega]_N^j = \zeta_{r,2;N}^j - \frac{h_N^j}{2\sqrt{\varepsilon}} \delta_t^\star \rho_N^j, \; j = 1, ..., M, \\ \omega_i^0 = -\rho_i^0, \; i = 0, ..., N. \end{cases} \tag{3.27}$$

Here we see that equation (3.26) is the same that we obtain when we analyse the

error component ρ in a stationary problem that is discretized using $\mathcal{L}_\varepsilon$ with Robin boundary conditions, and $\mathcal{X}^j_{1,i}, \zeta^j_{l,1;0}, \zeta^j_{r,1;N}$, the corresponding truncation errors (see Theorem 3.2.1). So, we can invoke the error bound of Theorem 3.2.1 to get

$$|\rho_i^j| \leq CN^{-2} \quad \text{for all } i, j. \tag{3.28}$$

Now we shall obtain a bound for the error component ω_i^j. Note that the problem (3.27) is similar to the discrete problem (3.5). Hence, using the discrete maximum principle (Lemma 3.1.1) we get

$$\begin{aligned} |\omega_i^j| &\leq C(\max_i |\rho_i^0| + \max_j |[D_l^{N,M}\omega]_0^j| + \max_j |[D_r^{N,M}\omega]_N^j| + \max_{i,j} |\mathcal{X}^j_{2;i} - \delta_t^\star \rho_i^j|) \\ &\leq C(\Delta t + N^{-2+\gamma} + \max_{i,j} |\delta_t^\star \rho_i^j|), \end{aligned} \tag{3.29}$$

where we have used the triangle inequality, the inequality in (3.28), and the fact that $\mathcal{X}^j_{2,i}, \zeta^j_{l,2;0}$, and $\zeta^j_{r,2;N}$ are bounded by $C(\Delta t + N^{-2+\gamma})$ for some $0 < \gamma < 1$ such that $N^{-\gamma} \leq C\Delta t$, which can be verified using Taylor expansion, standard interpolation error estimates, and (3.2). So, now it remains to bound the term $\delta_t^\star \rho_i^j$ in (3.29). Using (3.26), a straightforward calculation shows that $\delta_t^\star \rho_i^j$ satisfies

$$\begin{cases} [L_\varepsilon^{N,M} \delta_t^\star \rho]_i^j = \delta_t^\star \mathcal{X}^j_{1;i}, \ i = 1, ..., N-1, \\ [D_{l,x}^{N,M} \delta_t^\star \rho]_0^j = \delta_t^\star \zeta^j_{l,1;0}, \\ [D_{r,x}^{N,M} \delta_t^\star \rho]_N^j = \delta_t^\star \zeta^j_{r,1;N}. \end{cases} \tag{3.30}$$

To analyse the problem (3.30), we write the right hand side as

$$\begin{aligned}\delta_t^\star \mathcal{X}_{1;i}^j &= \frac{1}{\Delta t}\left[\mathcal{X}_{1;i}^j - \widetilde{\mathcal{X}}_{1;i}^{j-1}\right] \\ &= \frac{1}{\Delta t}\Bigg[\left([L_\varepsilon^{N,M} y]_i^j - (\mathcal{L}_\varepsilon y)_i^j\right) - \Bigg(\left([L_\varepsilon^{N,M} y]_{n-1}^{j-1} - (\mathcal{L}_\varepsilon y)_{n-1}^{j-1}\right)\psi_{n-1}(x_i^j) \\ &\qquad + \left([L_\varepsilon^{N,M} y]_n^{j-1} - (\mathcal{L}_\varepsilon y)_n^{j-1}\right)\psi_n(x_i^j)\Bigg)\Bigg],\end{aligned}$$

where

$$\psi_{n-1}(x) = \frac{x_n^{j-1} - x}{x_n^{j-1} - x_n^{j-1}} \text{ and } \psi_n(x) = \frac{x - x_{n-1}^{j-1}}{x_n^{j-1} - x_{n-1}^{j-1}} \text{ with } x_{n-1}^{j-1} \le x_i^j \le x_{n-1}^j \text{ for some } n.$$

Set $\check{\mathcal{L}}_\varepsilon y = -\varepsilon \frac{\partial^2 y}{\partial x^2}$ and suppose its discretization is $[\check{L}_\varepsilon^{N,M} Y]_i^j = -\varepsilon \delta_x^2 Y_i^j$. Now by using the fact that the linear interpolation error is $\mathcal{O}(N^{-2})$, we can write

$$|\delta_t^\star \mathcal{X}_{1,i}^j| \le \left|\frac{1}{\Delta t}\int_{t_{j-1}}^{t_j}\left[\check{L}_\varepsilon^{N,M}\frac{\partial y}{\partial t}(x_i^j,t) - \check{\mathcal{L}}_\varepsilon \frac{\partial y}{\partial t}(x_i^j,t)\right]dt\right| + CN^{-2}.$$

Thus, using the Peano kernel theorem [20, 125] and the bounds in (3.2), we get the same bound for $\delta_t^\star \mathcal{X}_{1;i}^j$ that we get for the corresponding truncation error for stationary problem. Similarly we can obtain also same bounds for $\delta_t^\star \zeta_{l,1;0}^j$ and $\delta_t^\star \zeta_{r,1;N}^j$. Hence, we get $\delta_t^\star \rho_i^j \le CN^{-2}$ for all i, j. Therefore, on combining (3.28) and (3.29) we get the desired result.

□

Remark 3.3.1. The assumption $N^{-\gamma} \le C\Delta t$ for some $0 < \gamma < 1$ used in the above theorem is for the theoretical proof only. However, in the numerical experiments there is no influence of this restriction on the parameter-robust convergence behavior. Such an assumption is common in the literature (see, e.g. [58]).

3.4 Numerical experiments

We now present the numerical experiments that we performed for two test examples to verify our theoretical result. To construct the adaptive mesh we use Algorithm 2. In the stopping criterion we have taken the value $\varrho = 1.1$. As the second derivative of the smooth part v is bounded independently of ε, in practice, it is observed that the monitor function with w replaced by y also produces similar layer-adapted meshes and numerical results [124].

Example 3.4.1. Consider the problem

$$\begin{cases} \frac{\partial y}{\partial t} - \varepsilon \frac{\partial^2 y}{\partial x^2} + \frac{1+x^2}{2} y = t^3, \quad (x,t) \in (0,1) \times (0,1], \\ \mathcal{D}_l y(0,t) = -\frac{128}{35} \pi^{-1/2} t^{7/2}, \ t \in (0,1], \\ \mathcal{D}_r y(1,t) = -\frac{128}{35} \pi^{-1/2} t^{7/2}, \ t \in (0,1], \\ y(x,0) = 0, \ x \in [0,1]. \end{cases}$$

The surface plot in Figure 3.1 displays the numerical solution of Example 3.4.1 for $\varepsilon = 10^{-4}$ with $N = 128$ and $M = 32$. This clearly shows the existence of boundary layers near $x = 0$ and $x = 1$. The exact solution of Example 3.4.1 is unknown, so the maximum pointwise errors and rates of convergence are calculated by using the double mesh principle. We bisect the meshes in space and time, and calculate the pointwise errors at the coarse mesh points using the formula

$$E_{i,k}^{\varepsilon,N,M} = |Y_{2i}^{2k,2N,2M} - Y_i^{k,N,M}|.$$

Algorithm 2: Algorithm for the adaptive mesh and adaptive solution

Input: $N,\ M \in \mathbb{N},\ 0 < \varepsilon \leq 1$ and $\varrho > 1$.

Output: Adaptive mesh $\{x_i^k\}$ and adaptive solution Y_i^k at each time level t_k.

1. **Initialization:** Initialize the mesh (for iteration $r = 1$) taking $\{x_i^{k,(r)}\}$ as the uniform mesh for $k = 1$, otherwise x^{k-1} for kth time level.

2. Solve the discrete problem (3.5) for $Y_i^{k,(r)}$ on $\{x_i^{k,(r)}\}$.

3. Find the discrete monitor function defined by

$$\mathcal{M}_i^{k,(r)} = \aleph^{k,(r)} + |\delta_x^2 Y_i^{k,(r)}|^{1/2}, \quad \text{for } i = 1, ..., N-1,$$

where $\aleph^{k,(r)}$ is defined by

$$\aleph^{k,(r)} = h_1^{k,(r)} |\delta_x^2 Y_1^{k,(r)}|^{1/2} + \sum_{i=2}^{N-1} h_i^{k,(r)} \left\{ \frac{|\delta_x^2 Y_{i-1}^{k,(r)}|^{1/2} + |\delta_x^2 Y_i^{k,(r)}|^{1/2}}{2} \right\} + h_N^{k,(r)} |\delta_x^2 Y_{N-1}^{k,(r)}|^{1/2}.$$

4. Set $H_i^{k,(r)} = h_i^{k,(r)} \left(\frac{\mathcal{M}_{i-1}^{k,(r)} + \mathcal{M}_i^{k,(r)}}{2} \right)$ for $i = 1, ..., N$, take $\mathcal{M}_0^{k,(r)} = \mathcal{M}_1^{k,(r)}$ and $\mathcal{M}_N^{k,(r)} = \mathcal{M}_{N-1}^{k,(r)}$. Then define $L_i^{k,(r)}$ by$L_i^{k,(r)} = \sum_{j=1}^{i} H_j^{k,(r)}$ for $i = 1, ..., N$ and $L_0^{k,(r)} = 0$.

5. **Stopping criterion**: Define $\varrho^{(r)}$ by $\varrho^{(r)} = \frac{N}{L_N^{k,(r)}} \max\limits_{i=1,...,N} H_i^{k,(r)}$. Go to Step 7 if $\varrho^{(r)} \leq \varrho$, else continue with Step 6.

6. Define $Z_i^{k,(r)} = i \frac{L_N^{k,(r)}}{N}$ for $i = 0, 1, ..., N$. New mesh $\{x_i^{k,(r+1)}\}$ is generated by evaluating the interpolant function of the points $(L_i^{k,(r)}, x_i^{k,(r)})$ at $Z_i^{k,(r)}$, set $r = r + 1$ and return to Step 2.

7. Take $\{x_i^{k,(r-1)}\}$ as the final layer-adaptive mesh and $Y_i^{k,(r-1)}$ as the required adaptive solution at the kth time level.

8. Go to Step 1 with $k = k + 1$, repeat the same process for the adaptive mesh and solution at $(k + 1)$th time level.

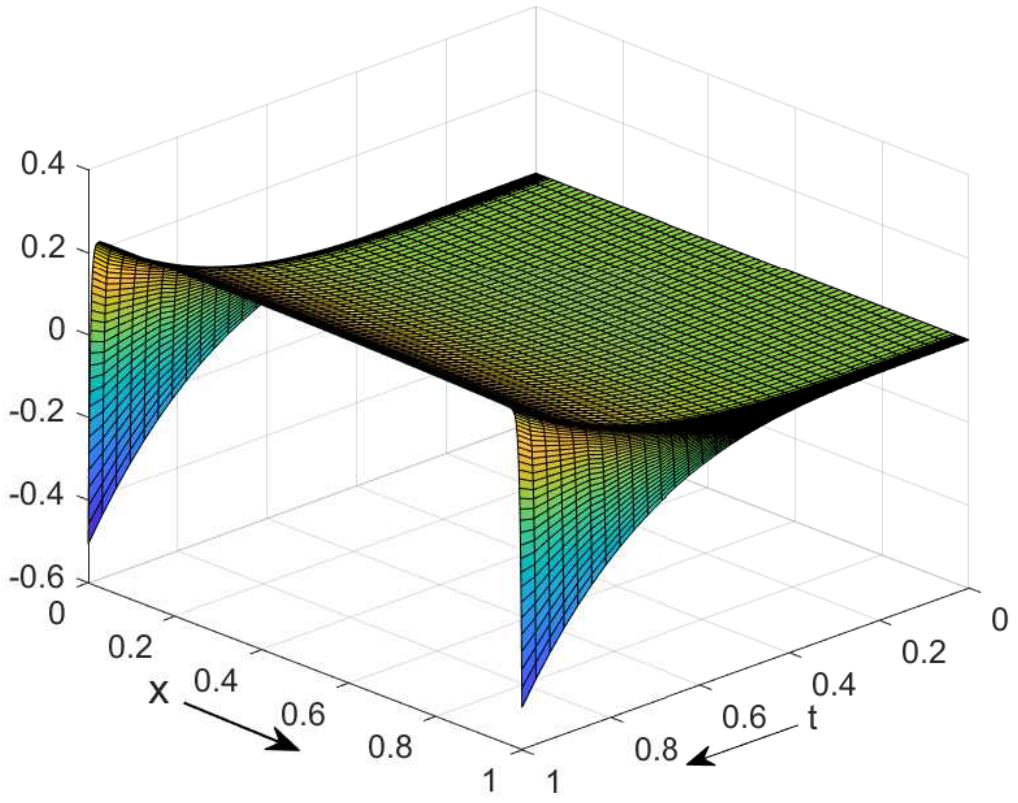

FIGURE 3.1: Surface plot of the numerical solution of Example 3.4.1 with $N = 128$, $M = 32$, and $\varepsilon = 10^{-4}$.

Using these values, the maximum pointwise errors and the parameter-robust errors are calculated by

$$E^{\varepsilon,N,M} = \max_{i,k} E^{\varepsilon,N,M}_{i,k} \quad \text{and} \quad E^{N,M} = \max_{\varepsilon} E^{\varepsilon,N,M},$$

respectively. We then calculate the rates of convergence and the parameter-robust rates of convergence by

$$F^{\varepsilon,N,M} = \log_2\left(\frac{E^{\varepsilon,N,M}}{E^{\varepsilon,2N,2M}}\right) \quad \text{and} \quad F^{N,M} = \log_2\left(\frac{E^{N,M}}{E^{2N,2M}}\right),$$

respectively. The numerical results for Example 3.4.1 are presented in Table 3.1.

TABLE 3.1: Errors and convergence rates for Example 3.4.1.

ε	$N = 32$ $M = 8$	$N = 64$ $M = 16$	$N = 128$ $M = 32$	$N = 256$ $M = 64$	$N = 512$ $M = 128$
10^{0}	3.2130e-02 0.9641	1.6470e-02 0.9827	8.3343e-03 0.9916	4.1915e-03 0.9958	2.1018e-03
10^{-1}	9.5181e-03 0.9209	5.0272e-03 0.9592	2.5857e-03 2.9895	2.1018e-03 1.6721	6.5953e-04
10^{-2}	2.4266e-02 1.0164	1.1996e-02 1.0099	5.9569e-03 1.0052	2.9678e-03 1.0027	1.4812e-03
10^{-3}	2.5267e-02 1.0246	1.2420e-02 1.0135	6.1519e-03 1.0071	3.0609e-03 1.0036	1.5266e-03
10^{-4}	2.5445e-02 1.0268	1.2489e-02 1.0144	6.1824e-03 1.0074	3.0754e-03 1.0038	1.5336e-03
10^{-5}	2.5488e-02 1.0274	1.2505e-02 1.0149	6.1883e-03 1.0077	3.0776e-03 1.0039	1.5346e-03
10^{-6}	2.5493e-02 1.0274	1.2507e-02 1.0149	6.1893e-03 1.0078	3.0780e-03 1.0039	1.5348e-03
10^{-7}	2.5495e-02 1.0275	1.2507e-02 1.0148	6.1897e-03 1.0078	3.0782e-03 1.0040	1.5348e-03
10^{-8}	2.5497e-02 1.0275	1.2508e-02 1.0149	6.1896e-03 1.0078	3.0782e-03 1.0040	1.5348e-03
$E^{N,M}$ $F^{N,M}$	3.2130e-02 0.9641	1.6470e-02 0.9827	8.3343e-03 0.9916	4.1915e-03 0.9958	2.1018e-03

From this table, we observe that the error is decreasing as the number of mesh points is increasing. Moreover, the rate of convergence is one. This is due to the fact that the time discretization errors are dominating the global errors in this case. In order to show the contribution of the space discretization errors to the global errors we calculate the following convergence rates

$$\widehat{F}^{\varepsilon,N,M} = \log_2\left(\frac{E^{\varepsilon,N,M}}{E^{\varepsilon,2N,4M}}\right) \quad \text{and} \quad \widehat{F}^{N,M} = \log_2\left(\frac{E^{N,M}}{E^{2N,4M}}\right).$$

Observe that the number of mesh points in space is doubled, whereas the number of

TABLE 3.2: Errors and convergence rates for Example 3.4.1.

ε	$N=32$ $M=8$	$N=64$ $M=32$	$N=128$ $M=128$	$N=256$ $M=512$	$N=512$ $M=2048$
10^{0}	3.2130e-02 1.9490	8.3210e-03 1.9877	2.980e-03 1.9969	5.2559e-04 1.9995	1.3143e-04
10^{-1}	9.5181e-03 1.8193	2.5657e-03 1.9801	6.5031e-04 2.0160	1.6078e-04 1.9829	4.0673e-05
10^{-2}	2.4266e-02 2.0283	5.9485e-03 2.0084	1.4783e-03 2.0024	3.6896e-04 2.0003	9.2221e-05
10^{-3}	2.5267e-02 2.0396	6.1456e-03 2.0108	1.5248e-03 2.0031	3.8039e-04 2.0007	9.5049e-05
10^{-4}	2.5445e-02 2.0418	6.1794e-03 2.0112	1.5329e-03 2.0030	3.8240e-04 2.0008	9.5546e-05
10^{-5}	2.5488e-02 2.0425	6.1871e-03 2.0117	1.5342e-03 2.0032	3.8272e-04 2.0011	9.5608e-05
10^{-6}	2.5493e-02 2.0423	6.1889e-03 2.0119	1.5345e-03 2.0032	3.8278e-04 2.0011	9.5627e-05
$E^{N,M}$ $\widehat{F}^{N,M}$	3.2130e-02 1.9490	8.3210e-03 1.9877	2.980e-03 1.9969	5.2559e-04 1.9995	1.3143e-04

mesh points in time is quadrupled. In this way, the contributions of time and space discretizations are balanced. The results are displayed in Table 3.2. From these results, we observe that the rate of convergence is two.

Example 3.4.2. Consider the problem

$$\begin{cases} \frac{\partial y}{\partial t} - \varepsilon \frac{\partial^2 y}{\partial x^2} + (1 + xe^{-t})y = f(x,t), \quad (x,t) \in (0,1) \times (0,1], \\ \mathcal{D}_l y(0,t) = \phi_l(t), \ t \in (0,1], \\ \mathcal{D}_r y(1,t) = \phi_r(t), \ t \in (0,1], \\ y(x,0) = 0, \ x \in [0,1], \end{cases}$$

where the functions $f(x,t)$, $\phi_l(t)$, and $\phi_r(t)$ are such that

$$y(x,t) = t\left(\frac{e^{-x/\sqrt{\varepsilon}} + e^{-(1-x)/\sqrt{\varepsilon}}}{1+e^{-1/\sqrt{\varepsilon}}} - \cos^2(\pi x)\right).$$

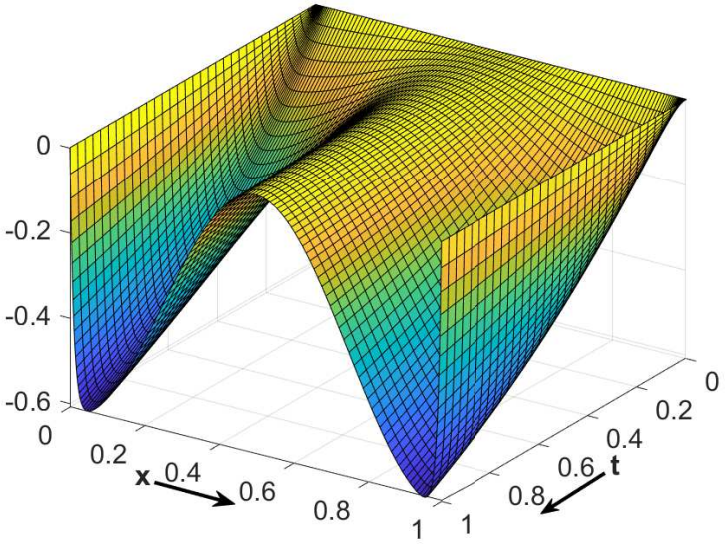

FIGURE 3.2: Surface plot of the numerical solution of Example 3.4.2 with $N = 128$, $M = 32$, and $\varepsilon = 10^{-4}$.

The surface plot in Figure 3.2 displays the numerical solutions of Example 3.4.2 for $\varepsilon = 10^{-4}$ with $N = 128$ and $M = 32$. This clearly shows the existence of boundary layers near $x = 0$ and $x = 1$. We calculate the pointwise errors using the formula

$$E_{i,k}^{\varepsilon,N,M} = |Y_i^k - y(x_i^k, t_k)|.$$

After that the errors $E^{\varepsilon,N,M}$ and $E^{N,M}$, and convergence rates $F^{\varepsilon,N,M}$ and $F^{N,M}$ are computed as described earlier. Table 3.3 displays the numerical results for Example 3.4.2, where the last two rows represents the parameter-robust errors and the parameter-robust rates of convergence. In this table, observe that N and M are

TABLE 3.3: Errors and convergence rates for Example 3.4.2.

ε	$N = 32$ $M = 8$	$N = 64$ $M = 16$	$N = 128$ $M = 32$	$N = 256$ $M = 64$	$N = 512$ $M = 128$
10^{0}	1.5235e-03 1.9610	3.9133e-04 1.9609	1.0052e-04 2.0012	2.5109e-05 1.9998	6.2779e-06
10^{-1}	1.3209e-03 1.9814	3.3450e-04 1.9804	8.4770e-05 2.0005	2.1185e-05 1.9999	5.2967e-06
10^{-2}	2.5805e-03 2.0394	6.2775e-04 2.0115	1.5569e-04 2.0048	3.8792e-05 2.0015	9.6878e-06
10^{-3}	7.8877e-03 1.9513	2.0397e-03 2.1140	4.7116e-04 2.0394	1.1462e-04 2.0117	2.8424e-05
10^{-4}	1.3994e-02 2.1202	3.2189e-03 2.0744	7.6427e-04 2.0154	1.8904e-04 1.9678	4.8325e-05
10^{-5}	1.9291e-02 2.2567	4.0366e-03 2.0561	9.7065e-04 2.0389	2.3620e-04 2.0079	5.8728e-05
10^{-6}	2.3577e-02 2.3757	4.5430e-03 2.1066	1.0548e-03 2.0267	2.5887e-04 2.0165	6.3981e-05
10^{-7}	2.7531e-02 2.5183	4.8054e-03 2.1227	1.1034e-03 2.0438	2.6761e-04 2.0172	6.6108e-05
10^{-8}	2.8902e-02 2.4555	5.2693e-03 2.2264	1.1260e-03 2.0497	2.7197e-04 2.0215	6.6985e-05
$E^{N,M}$ $F^{N,M}$	2.8902e-02 2.4555	5.2693e-03 2.2264	1.1260e-03 2.0497	2.7197e-04 2.0215	6.6985e-05

increasing with the same ratio. From this table, we can deduce that the rate of convergence is two. Note that in this case the space discretization errors are dominating the global errors.

In summary, we observe that the proposed numerical method is parameter-robust convergent of order two in space and order one in time. Further, the assumption $N^{-\gamma} \leq C\Delta t$ is not necessary in practice.

At the first time level t_1, we have shown the adaptive movement of spatial mesh points for Examples 3.4.1 and 3.4.2 in Figures 3.3 and 3.4, respectively. These

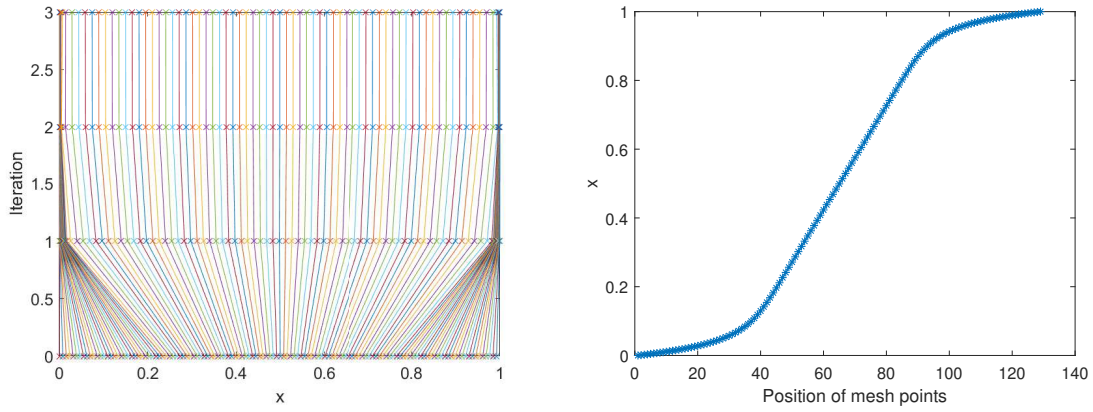

FIGURE 3.3: Mesh trajectory and position of space mesh points taking $N = 128$, $M = 32$, and $\varepsilon = 10^{-5}$ for Example 3.4.1.

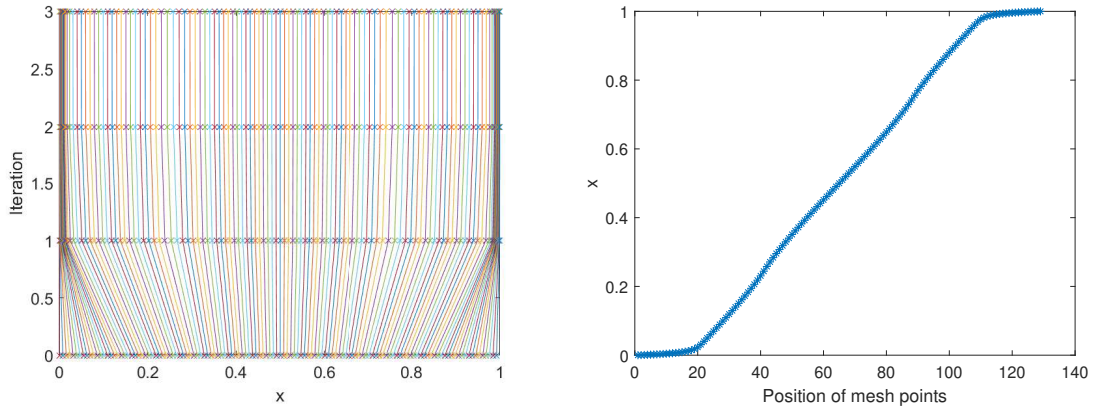

FIGURE 3.4: Mesh trajectory and position of space mesh points taking $N = 128$, $M = 32$, and $\varepsilon = 10^{-5}$ for Example 3.4.2.

figures display the condensation of mesh points towards the boundary layers in few iterations and finally the adaptation of solution behavior by itself. In Figure 3.5, we have plotted the log-log graphs of the maximum pointwise errors versus the number of spatial mesh points N for both test examples. The slopes of these plots also validate the theoretically obtained convergence result in space.

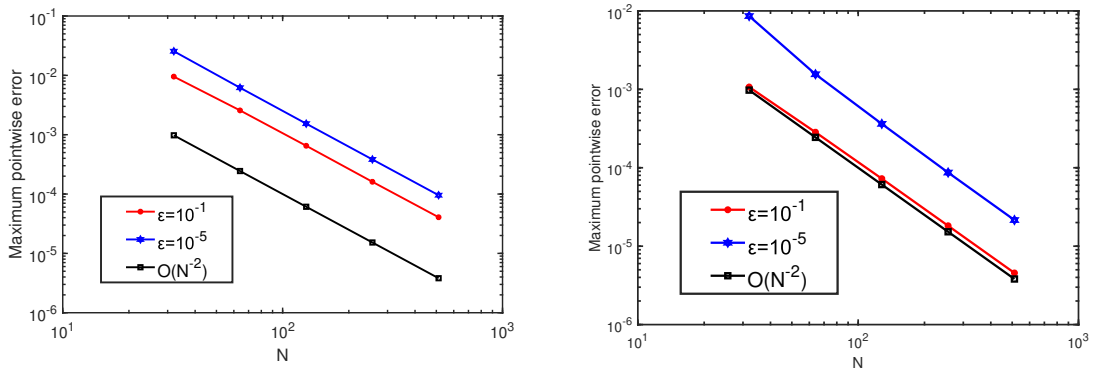

FIGURE 3.5: Log-log plots of the maximum pointwise error for Examples 3.4.1 (left) and 3.4.2 (right).

3.5 Conclusions

A parameter-robust adaptive numerical method is introduced for a class of singularly perturbed parabolic reaction-diffusion problems with RBCs. The adaptive mesh in spatial direction is generated using the equidistribution principle. The method is proved to be parameter-robust convergent of order two in space and order one in time. The theoretical error bound is supported by the numerical results.

****